

University of Dayton

eCommons

---

Graduate Theses and Dissertations

Theses and Dissertations

---

2007

## Synthesis, characterization, DNA binding and photoactivity of diruthenated CIS-5, 10-(4-pyridyl)-15, 20-(Pentafluorophenyl)porphyrin

Sandya Rani Beeram  
*University of Dayton*

Follow this and additional works at: [https://ecommons.udayton.edu/graduate\\_theses](https://ecommons.udayton.edu/graduate_theses)

---

### Recommended Citation

Beeram, Sandya Rani, "Synthesis, characterization, DNA binding and photoactivity of diruthenated CIS-5, 10-(4-pyridyl)-15, 20-(Pentafluorophenyl)porphyrin" (2007). *Graduate Theses and Dissertations*. 1468.  
[https://ecommons.udayton.edu/graduate\\_theses/1468](https://ecommons.udayton.edu/graduate_theses/1468)

This Thesis is brought to you for free and open access by the Theses and Dissertations at eCommons. It has been accepted for inclusion in Graduate Theses and Dissertations by an authorized administrator of eCommons. For more information, please contact [mschlangen1@udayton.edu](mailto:mschlangen1@udayton.edu), [ecommons@udayton.edu](mailto:ecommons@udayton.edu).

SYNTHESIS, CHARACTERIZATION, DNA BINDING AND PHOTOACTIVITY  
OF DIRUTHENATED C/S-5, 10-(4-PYRIDYL)-15, 20-  
(PENTAFLUOROPHENYL)PORPHYRIN

Thesis

Submitted to

The College of Arts and Sciences of the

UNIVERSITY OF DAYTON

in Partial Fulfillment of the Requirements for

The Degree

Master of Science in Chemistry

by

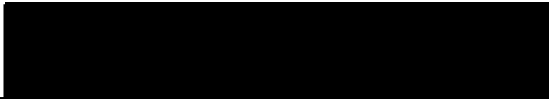
Sandya Rani, Beeram

UNIVERSITY OF DAYTON

Dayton, Ohio

December, 2007

APPROVED BY:



---

Shawn M. Swavey, Ph. D., Assistant Professor  
Committee Chair



---

Kevin M. Church, Ph.D., Associate Professor  
Committee Member



---

Gary W. Morrow, Ph.D., Professor  
Committee Member

## DEDICATION

To my father  
who should have lived  
to see this thesis

## ABSTRACT

SYNTHESIS, CHARACTERIZATION, DNA BINDING AND PHOTOACTIVITY OF DIRUTHENATED *CIS*-5,10-(4-PYRIDYL)-15, 20-(PENTAFLUOROPHENYL) PORPHYRIN.

Beeram Sandya Rani

University of Dayton

Advisor: Dr. Shawn. M. Swavey

The porphyrin 5,10-(4-pyridyl)-15,20-(pentafluorophenyl)porphyrin (I) was synthesized by refluxing a solution of pentafluorobenzaldehyde, 4-pyridinecarboxaldehyde and pyrrole in propionic acid. The separation of *cis*-porphyrin (I) from a mixture of six porphyrins was achieved by column chromatography. The porphyrin [5,10-(4-pyridyl)-15,20-(pentafluorophenyl)porphyrin Ru<sub>2</sub>(bipy)<sub>4</sub>Cl<sub>2</sub>](PF<sub>6</sub>)<sub>2</sub> (II) was synthesized by reacting *cis*-porphyrin (I) with *cis*-Ru(bipy)<sub>2</sub>Cl<sub>2</sub> in glacial acetic acid. Electronic transitions associated with *cis*-porphyrin (I) consist of an intense Soret band at 410 nm and three Q bands from 500-650 nm. Coordination of [Ru(bipy)<sub>2</sub>Cl]<sup>+</sup> groups to the pyridyl nitrogens of the porphyrin give additional electronic transitions associated with bipy orbitals and metal to ligand charge transfer (MLCT) transitions attributed to Ru(II) and

bipy orbitals. The cyclic voltammogram of *cis*-porphyrin (I) shows two quasireversible redox couples in the cathodic region which occur at  $E_{1/2} = -0.86$  V and  $-1.26$  V versus Ag/AgCl reference which are shifted to slightly more positive potentials when the porphyrin is coordinated to the Ru(II) groups. Ruthenium porphyrin (II) shows a quasireversible redox couple in the anodic region at  $0.83$  V versus Ag/AgCl attributed to  $\text{Ru}^{(\text{III/II})}$  couple. Spectroscopic titrations were performed with calf thymus DNA to determine a binding constant ( $K_b$ ) for *cis*-porphyrin (I) and ruthenium porphyrin (II): A binding constant of  $7.6 \times 10^5 \text{ M}^{-1}$  was determined for ruthenium porphyrin (II) and a value of  $2.0 \times 10^4 \text{ M}^{-1}$  was determined for the *cis* porphyrin (I). Irradiation of aqueous buffered solutions of circular plasmid DNA and the ruthenium porphyrin (II) complex with a 50 W tungsten-halogen lamp indicate, by gel electrophoresis, that light induced DNA photocleavage occurs.

## ACKNOWLEDGEMENTS

First of all I wish to thank my research advisor Dr. Shawn M. Swavey who made this thesis possible and guided me the whole time in graduate school. I should thank him for the training, support, advice and patience. His friendly and objective attitude made my study enjoyable and successful. He spent a great deal of his priceless time reading and correcting my Master thesis. I am particularly indebted to my parents and my brother for my upbringing and for the support of my receiving high education. I would not accomplish anything without them. I would like to thank my husband who is always supportive and I feel indebted for his caring and love. I want to sincerely thank my in-laws in India who through their love and support certainly made things easier for me and helped me to cope with a new culture of life in United States. I would like to thank University of Dayton, Chemistry department for giving me this excellent opportunity. Finally and equally I would like to thank all the faculty and staff for their support during my graduate study.

## TABLE OF CONTENTS

ABSTRACT.....	iii
ACKNOWLEDGEMENTS.....	v
LIST OF ILLUSTRATIONS.....	viii
LIST OF TABLES.....	x
LIST OF SYMBOLS/ABBREVIATIONS.....	xi
CHAPTER	
I. INTRODUCTION.....	1
II. EXPERIMENTAL SECTION.....	14
Materials.....	14
Solution electrochemistry .....	14
Electronic electrochemistry.....	15
Proton NMR Spectroscopy.....	15
Synthesis.....	15
DNA interactions.....	18
III. RESULTS AND DISCUSSION.....	22
Synthesis and characterization.....	22
Electronic absorption spectroscopy.....	25
Solution electrochemistry.....	27



IV. DNA INTERACTIONS.....	30
Photocleavage of circular plasmid DNA.....	33
V. CONCLUSIONS.....	38
VI. FUTURE EXPERIMENTS.....	39
VII. BIBLIOGRAPHY.....	40

## LIST OF ILLUSTRATIONS

1. Early photosensitizers.....	1
2. Jablonski diagram.....	2
3. The basic chemical structures of porphyrins, chlorins and bacteriochlorins.....	5
4. Structure of m-tetra hydroxyl phenyl chlorin.....	6
5. Structure of Verteporfin.....	7
6. Structure of phthalocyanines.....	7
7. 5-Aminoleavulinic acid (ALA) and Protoporphyrin IX.....	8
8. Porphine: The parent form of tetrapyrrolic macrocycle.....	9
9. Structure of tetra-pentafluorophenyl pophyrin.....	10
10. Early octahedral DNA probes.....	11
11. Intercalating ligands.....	12
12. Structures of porphyrin and its ruthenium analog in this study.....	13
13. Synthesis of 5,10-(4-pyridyl)-15,20-(pentafluorophenyl)porphyrin.....	22
14. Six different porphyrins resulted by reacting two different aldehydes with pyrrole in propionic acid.....	23
15. Synthesis of [5,10-(4-pyridyl)-15,20-(pentafluorophenyl)porphyrin- Ru <sub>2</sub> (bipy) <sub>4</sub> Cl <sub>2</sub> ] <sup>2+</sup> .....	24
16. Electronic absorption spectra in acetonitrile at room temperature for <i>cis</i> porphyrin (red) and ruthenium porphyrin (blue).....	26

17. Cyclic voltammograms of <i>cis</i> porphyrin (red) and ruthenium porphyrin (blue) in TBAPF <sub>6</sub> /Acetonitrile vs Ag/AgCl.....	29
18. Absorption spectra of pH 7.16 buffer solutions of ruthenium porphyrin (II) in the presence of increasing amounts of CT-DNA.....	31
19. Plot of [DNA]/( $\epsilon_a - \epsilon_f$ ) versus [DNA].....	32
20. Gel electrophoresis results of circular plasmid DNA (pUC18) in the presence of ruthenium porphyrin and without ruthenium porphyrin irradiated with 50 W quartz tungsten halogen lamp.....	35
21. Gel electrophoresis results both in the absence and presence of light.....	36

## LIST OF TABLES

1. Electronic absorption spectroscopy results for *cis* porphyrin and ruthenium  
Porphyrin.....27
2. Redox potentials and their assignments for *cis* porphyrin and ruthenium  
porphyrin.....28

## LIST OF ABBREVIATIONS

PDT.....	Photodynamic therapy
ROS.....	Reactive oxygen species
FDA.....	Food Drug administration
HVD.....	Hydroxy ethyl vinyl deuteron porphyrin
Pp.....	Protoporphyrin
ALA.....	5-Amino laevulinic acid
HpD.....	Hematoporphyrin derivative
DNA.....	deoxyribo nucleic acid
dppz.....	dipyrido[3,2-a:2',3'-c]phenazine
TAP.....	1,4,5,8-tetraazaphenanthrene
HAT.....	1,4,5,8,9,12-hexaazatriphenylene
dpb.....	2,3-bis(2-pyridyl)-benzo quinoxaline
TBAPF <sub>6</sub> .....	tetrabutyl ammonium hexafluorophosphate
DMF.....	N,N'- dimethyl formamide
CH <sub>3</sub> CN.....	Acetonitrile
NMR.....	Nuclear magnetic resonance
CDCl <sub>3</sub> .....	Deuterated chloroform
TMS.....	Tetramethylsilane
UV-Vis.....	Ultraviolet visible

CT..... Calf thymus  
DMSO.....Dimethyl sulfoxide  
BP.....Base pairs  
R<sub>f</sub>.....Retention factor  
<sup>1</sup>H NMR.....Proton NMR  
MLCT.....Metal to ligand charge transfer  
CV.....Cyclic voltammetry

## CHAPTER 1

### INTRODUCTION

There has been a growing interest in Photodynamic therapy (PDT) as a treatment modality to destroy cancer cells.<sup>1</sup> The first clinical application of PDT occurred in 1900 when Oscar Rabb, a medical student working with professor Herman von Tappeiner noted that paramecium caudatum cells died quickly when exposed to light in the presence of acridine orange.<sup>2</sup> In 1903, Jesionek and Tappeiner treated skin cancer with light and eosin.<sup>3</sup> In these instances acridine orange and eosin act as photosensitizers. In 1913, Meyer-Betz observed the photosensitizing effects of porphyrins in man by injecting himself intravenously with hematoporphyrin and noticed pain and swelling in the light exposed area.<sup>4</sup> The structures of the early photosensitizers are illustrated in Figure 1.

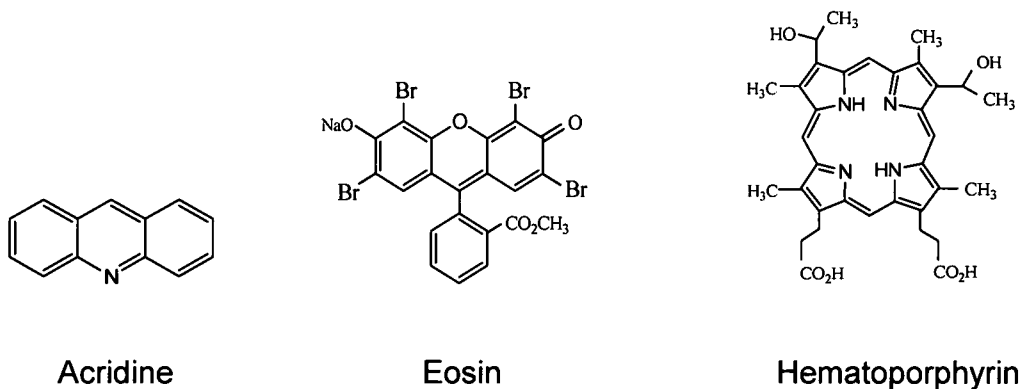


**Figure 1:** Early photosensitizers.

The uptake of porphyrins in significant amounts by tumors was first visualized by Policard in 1924 when he observed the characteristic red fluorescence of hematoporphyrin in experimental rat sarcoma illuminated with ultraviolet light.<sup>5</sup> Together with Jadlbauer, von Tappeiner went on to demonstrate the requirement of oxygen in photosensitization reactions and in 1907 introduced the term "photodynamic action" to describe the phenomenon.<sup>6</sup>

Three fundamental requirements for PDT are light, molecular oxygen and a photosensitizer. Each factor is harmless by itself but the combination of all three factors can result in the production of lethal cytotoxic agents that can destroy cancer cells.<sup>1</sup>

#### REACTION MECHANISMS OF PDT:

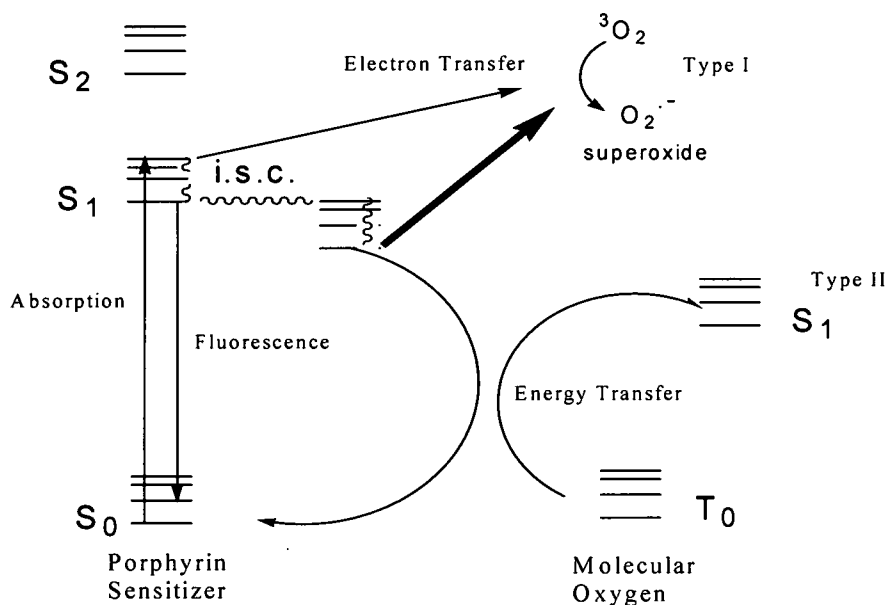


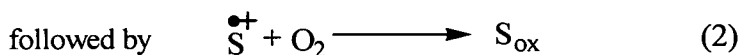
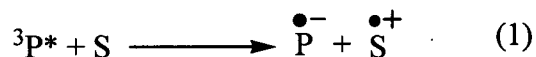
**Figure 2:** Jablonski diagram.



The photochemical and photophysical principles of PDT are schematically represented in the modified Jablonski diagram, (Figure 2).<sup>7</sup> The photosensitizer has no effect on the tissue unless it is activated by light of an appropriate wavelength. The photosensitizer absorbs a photon of energy from the light source. Once it has absorbed energy the excited photosensitizer can return to the ground state by a number of pathways. A good photosensitizer at this stage undergoes intersystem crossing to get rapidly converted to the long lived triplet state. There are two mechanisms by which the triplet state photosensitizer can react with biomolecules; these are known as the Type I and Type II reactions. In Type I reactions there might be an hydrogen atom abstraction or electron transfer reaction between the excited state of the sensitizer and the substrate to yield radicals and radical ions. Since these radical species are highly reactive they can interact with molecular oxygen to generate reactive oxygen species (ROS) such as superoxide anion, hydrogen peroxide and hydroxyl radicals. Type II reactions produce an excited and highly reactive state of oxygen known as singlet oxygen. Direct interaction of the excited triplet state photosensitizer with molecular oxygen results in formation of reactive singlet oxygen. Singlet oxygen and ROS are oxidizing molecules that can readily react with biological molecules and they can oxidatively modify selected amino-acid residues, unsaturated lipids or damage DNA.<sup>8</sup> Type II reactions are reported to dominate during PDT. However Type I reactions may become more dominant under conditions where photosensitizers are highly concentrated, and especially under hypoxic conditions.<sup>9</sup> These reaction types are illustrated in scheme 1.

## Scheme 1: Type I and Type II Reactions

### Type I Reactions:

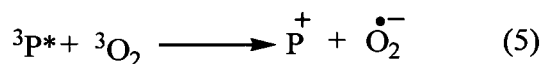


or



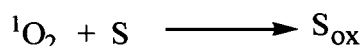
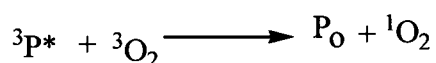
In both cases giving an oxidized biomolecule  $\text{S}_{\text{ox}}$ .

An alternate type I reaction pathway might be



Reaction (4) may follow after reaction (5) and reaction (2) may follow after reaction (6).

### Type II Reactions:



The first sensitizer used in clinical PDT was a Hematoporphyrin derivative and its purified fraction Photofrin HpD. Photofrin<sup>®</sup> has passed the clinical trials and it was the first PDT agent approved by FDA for treating esophageal cancer and is currently used to treat a wide variety of cancers.<sup>10</sup> Photofrin<sup>®</sup> is a mixture containing hematoporphyrin, hydroxyl ethyl vinyl deuterium porphyrin (HVD) and

protoporphyrin (Pp) as well as complex dimeric and oligomeric fractions.<sup>11</sup> It has low quantum yields and low efficiency in the generation of reactive oxygen species. It results in prolonged skin photosensitivity lasting for 6-8 weeks.<sup>12</sup> It is excited with red light at 630 nm. This wavelength can penetrate tissue to a depth of few mm and hence is unsuitable for treating deep seated tumors. New photosensitizers, so called "second generation" photosensitizers have been synthesized that have better properties than Photofrin®. Chlorins and Bacteriochlorins are a group of molecules very similar to porphyrins which were found to be effective photosensitizers in cancer prevention.<sup>13</sup> In chlorins one of the exopyrrole double bonds of the porphyrin ring is hydrogenated and in bacteriochlorins, two of the exopyrrole double bonds of the porphyrin ring are hydrogenated thus enabling maximum absorption at longer wavelengths. The core structures of porphyrin, chlorin and bacteriochlorin are illustrated in Figure 3.

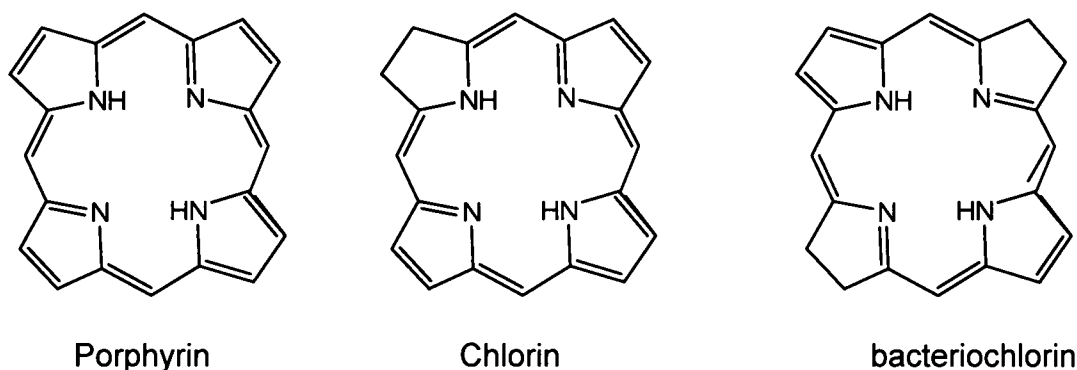


**Figure 3:** The basic chemical structures of porphyrins, chlorins and bacteriochlorins.

Temoporfin or tetra (m- hydroxyl-phenyl) chlorin, Figure 4 under the trade name Foscan<sup>TM</sup> is a potent photosensitizer available for clinical use at present. This drug was approved by the European Union for the treatment of head and neck cancers in 2001. It is 200 times more effective than Photofrin<sup>®</sup>. It is activated with a longer wavelength and lower light intensity compared to Photofrin<sup>®</sup> and also has a longer half life in the triplet state generating more cytotoxic oxygen species.<sup>14</sup> Foscan is also in clinical trials for late stage esophageal cancer and dysplasia in Barrett's esophagus.<sup>15</sup> It is more selective between tumor and normal tissue.

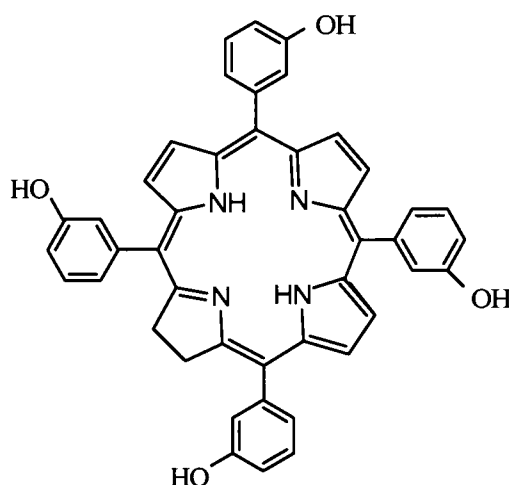


**Figure 4:** Structure of m-tetra hydroxyl phenyl chlorin.

Verteporfin (benzo-porphyrin-derivative mono-acid ring A), Figure 5, which is a chlorin type molecule under the trade name Visudyne<sup>TM</sup> is in Phase III clinical trials for cutaneous non-melanoma skin cancer and Phase I/II trials against non-melanoma skin cancers (such as multiple non-melanoma skin cancer)<sup>16</sup>, psoriasis<sup>17</sup> and psoriatic and rheumatoid arthritis. It has rapid tumor accumulation and reduced skin photosensitivity.<sup>18</sup>

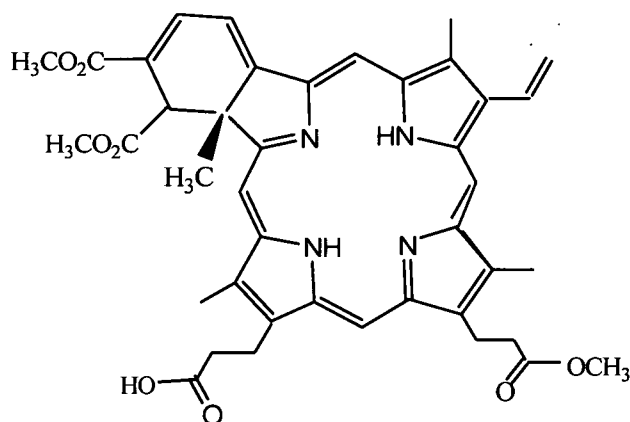


**Figure 5:** Structure of Verteporfin.

Pthalocyanines have emerged to be a promising class of second generation photosensitizers.<sup>19</sup> The core consists of a tetra pyrrole unit, but in contrast to porphyrin, the pyrrole subunits are linked by nitrogen atoms rather than by methine bridges. This causes absorption spectrum to shift to longer wavelengths and hence increased tissue penetration.<sup>20</sup> Incorporation of diamagnetic metals (Zn, Al) enables longer triplet state life times increasing the efficiency of the formation of reactive oxygen species. The basic structure of pthalocyanines is represented in Figure 6.

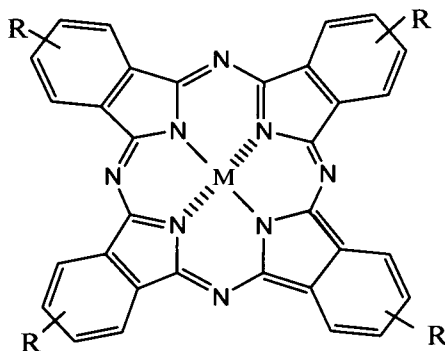


**Figure 6:** Structure of pthalocyanines.



region in the neighbourhood of 400 nm (called the **Soret band**). In 1884, Nencki isolated the first pure porphyrin by preparing Hematoporphyrin hydrochloride directly from isolated heme.<sup>23</sup> In 1912, Kuster first proposed the structure of porphyrins as four pyrrole units linked by four methine bridges.<sup>24</sup> The parent form of these tetrapyrrolic macrocycles is known as “porphine”, Figure 8.

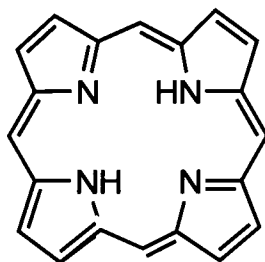


**Figure 8:** Porphine: The parent form of tetrapyrrolic macrocycle.

In 1975, Dougherty demonstrated HpD could selectively destroy tumors upon irradiation.<sup>25</sup> Porphyrins were used as ideal photosensitizers because they generate singlet oxygen and have maximum absorption in the red portion of the electromagnetic spectrum which results in maximum penetration of light into the tissue.<sup>8</sup> Most porphyrinoid photosensitizers have more than one absorption band and hence are used for tissue depth controlled penetration. In order to increase the quantum efficiency of photosensitizers such as porphyrins, fluorinated porphyrin derivatives, Figure 9 have been used. Enhanced triplet quantum yields are observed for fluorinated porphyrins which make them ideally suited to act as photosensitizers in photodynamic therapy.<sup>26</sup> In addition to increased quantum efficiency pentafluorophenyl substituents have been utilized to covalently link sugars to porphyrins which improves the cell uptake.<sup>27</sup>

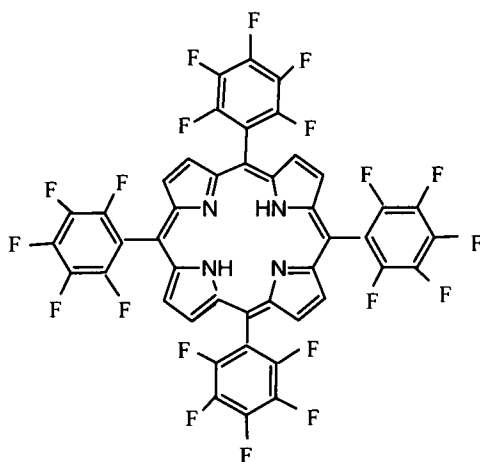


**Figure 9:** Structure of tetra-pentafluorophenyl porphyrin.

Metal complexes represent a promising field in the discovery of new PDT agents since they react with double stranded DNA directly from their excited state<sup>28,29</sup> or via the production of various reactive species such as  $\text{OH}^\bullet$ ,  $\text{O}_2^-$  or  $^1\text{O}_2$ .<sup>30,31,32</sup> Some examples of metal complexes that cleave DNA upon irradiation include mono nuclear  $\text{Re(I)}^{33}$ ,  $\text{Ru(II)}^{28}$ , and  $\text{Rh(III)}^{34}$  complexes, dinuclear rhodium(II,II)<sup>35</sup> and trinuclear  $\text{Ru(II)-Rh(III)-Ru(II)}^{36}$  complexes. The three main properties that make ruthenium complexes well suited to medicinal application are their rate of ligand exchange, range of accessible oxidation states and the ability of ruthenium to mimic iron in binding to certain biological molecules.<sup>37</sup> Intercalators are small molecules that contain a planar aromatic heterocyclic functionality which can insert and stack between the base pairs of double helical DNA.<sup>38</sup> The early studies describing the intercalation of coordinatively saturated octahedral transition-metal complexes with DNA focused on the binding of tris(phenanthroline) complexes of zinc, cobalt and ruthenium to DNA, Figure 10.<sup>39</sup> Studies with these simple metal complexes provided a basis for



understanding how octahedral complexes might interact noncovalently with DNA and also for exploring how the photophysical and redox characteristics of the metal complexes might be utilized in developing new probes for DNA.

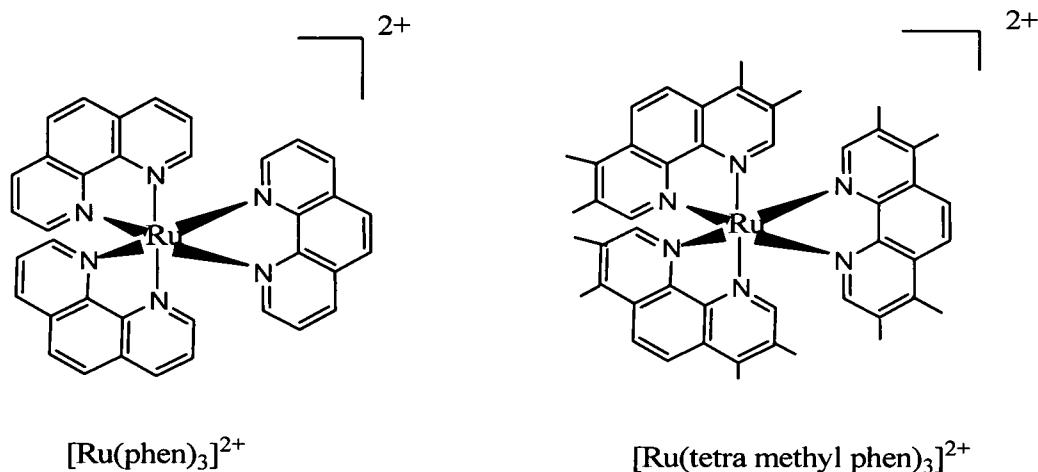
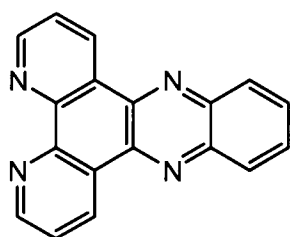
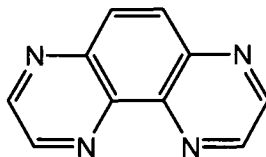


**Figure 10:** Early octahedral DNA probes.

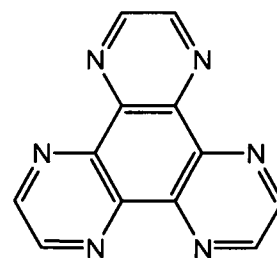
Increasing the surface area for intercalative stacking by a complex leads to an increase in intercalative binding affinity. Bipyridyl and phenanthroline complexes of ruthenium containing the dipyrido[3,2-a:2',3'-c]phenazine (dppz) ligand show good intercalation into the DNA.<sup>40</sup> The dppz complexes, with their large aromatic surface area show extremely high affinity for DNA, with binding constants  $> 10^6 \text{ M}^{-1}$ .<sup>41</sup> Analogous ruthenium complexes, with 1,4,5,8-tetraazaphenanthrene (TAP), 1,4,5,8,9,12-hexaazatriphenylene (HAT) also interact with DNA and like dppz complexes, show changes in photophysical properties upon binding to the DNA duplex.<sup>42</sup> Bimetallic complexes bridged by the 2,3-bis(2-pyridyl)-benzo quinoxaline (dpb) ligand have also been shown to bind to DNA by intercalation.<sup>43</sup> The structures of dppz, TAP, HAT and dpb are illustrated in the Figure 11.



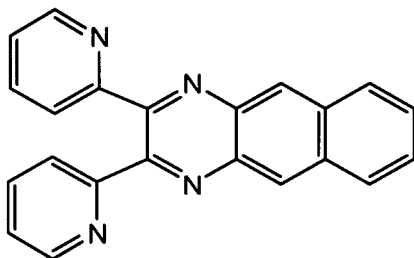
dppz



TAP



HAT



dpb

**Figure 11:** Intercalating ligands.

Porphyrrins containing meso substituted pyridyl groups are very well suited to coordinate metal complexes at the porphyrin periphery.<sup>44</sup> The advantages of using polypyridyl ruthenium (II) substituents covalently linked to porphyrins are the added water solubility and the ability of ruthenium (II) polypyridyl complexes to intercalate and oxidize DNA bases resulting in decomposition.<sup>45</sup> The present thesis describes the synthesis of 5,10-(4-pyridyl)-15,20-(pentafluorophenyl)porphyrin [Figure 12(I)] and its ruthenium (II) analog [Figure 12(II)]. Characterization of these complexes is accomplished by UV-Vis spectroscopy, cyclic voltammetry, <sup>1</sup>H NMR, time-of-flight mass spectrometry and elemental analysis. UV-Vis titrations of these porphyrins with calf thymus (CT) DNA were performed to determine the binding constant. Agarose gel

electrophoresis was performed to determine the photocleavage of circular plasmid (pUC18) DNA by ruthenium porphyrin [Figure 12(II)] after irradiation with a 50 W tungsten-halogen lamp.

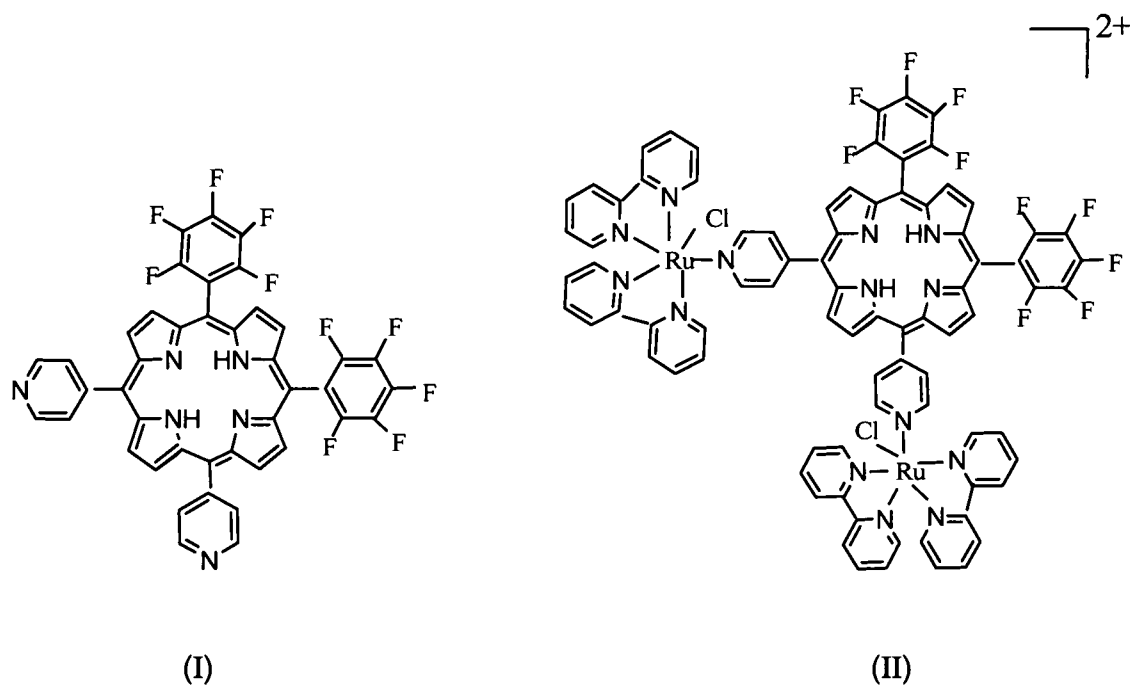


**Figure 12:** Structures of porphyrin and its ruthenium analog in this study.

## CHAPTER 2

### EXPERIMENTAL SECTION

#### **Materials**

All reagents were analytical grade unless mentioned otherwise. 4-pyridinecarboxaldehyde, pentafluorobenzaldehyde, propionic acid, tetrabutyl ammonium hexafluorophosphate,  $\text{TBAPF}_6$ , used as supporting electrolyte for electrochemistry and acetonitrile (extra dry < 50 ppm water) for electrochemistry were purchased from Acros Organics. Ammonium hydroxide, N,N'-dimethyl formamide (DMF), methanol, acetonitrile, diethyl ether, methylene chloride, ethanol, sea sand, glacial acetic acid and ethyl acetate were used from Fisher Scientific. (60-200 mesh) silica gel was obtained from Sorbent Technologies. Ruthenium (III) chloride trihydrate and 2,2'-bipyridine were obtained from Aldrich. Pyrrole (Aldrich) was vacuum distilled prior to use and all other reagents were used without further purification. Elemental analyses were performed by Atlantic Microlab, Norcross, Ga. High resolution mass spectroscopy was performed at the Mass Spectrometry and Proteomics facility, The Ohio State University.

#### **Solution Electrochemistry**

Solution cyclic voltammograms were recorded using a one compartment, three electrode cell, (model 630A Electrochemical analyzer from CH-Instruments)

equipped with a platinum wire auxillary electrode. The working electrode was a 2.0 mm diameter glassy carbon electrode from CH-Instruments. The working electrode was polished initially using 0.30  $\mu$  followed by 0.05  $\mu$  alumina polish (CH-Instruments) and then sonicated in distilled water for 5 sec prior to use. Potentials were referenced to a Ag/AgCl electrode, CH-Instruments. The supporting electrolyte was 0.1 M tetrabutyl ammonium hexafluorophosphate (TBAPF<sub>6</sub>) and the measurements were made in extra dry, < 50 ppm water, acetonitrile.

### Electronic Spectroscopy

UV-Vis spectra were recorded at room temperature using a Shimadzu 1501 photodiode array Spectrophotometer with 2 nm resolution. Samples were run in UV-grade CH<sub>3</sub>CN in 1 cm quartz cuvettes.

### Proton NMR Spectroscopy

<sup>1</sup>H NMR spectra were recorded on a Bruker 300 MHz spectrophotometer using deuterated chloroform (CDCl<sub>3</sub>) as the solvent and tetramethylsilane (TMS) as the internal standard.

### Synthesis

#### *cis*-Ru(bipy)<sub>2</sub>Cl<sub>2</sub><sup>46</sup>

Bipyridine (3.00 gm, 19.0 mmoles) was dissolved initially in 15 mL of DMF and 2.80 gm (66.5 mmoles) of lithium chloride was added followed by 2.50 gm (9.50 mmoles) of RuCl<sub>3</sub>·3H<sub>2</sub>O and the reaction mixture was heated at reflux for 8

hours. The mixture was cooled to room temperature and poured into rapidly stirred 50 mL of acetone and the flask was rinsed with 2×12 mL portions of acetone. The mixture was cooled overnight and filtered giving a black/red powder which was sonicated in approximately 50 mL water and filtered again giving a microcrystalline powder which was washed with water until the filtrate was no longer orange followed by 3×20 mL diethyl ether and air dried. The product yield was 1.60 g (9.50 mmoles, 51 % yield).

5,10-(4-pyridyl)-15,20-(pentafluorophenyl)porphyrin [(cis- H<sub>2</sub>(DPyFP))]

A solution containing 1.9 mL (15 mmoles) of pentafluorobenzaldehyde and 4.3 mL (45 mmoles) 4-pyridine carboxaldehyde in 100 mL of propionic acid was heated at reflux for 5 min. Freshly distilled pyrrole (4.2 mL, 60 mmoles) was added to this solution and the reaction mixture was heated at reflux for 2 hr. Upon cooling to room temperature the solution was divided into two fractions and each fraction was neutralized by cautious addition to a 100 mL 50:50 methanol/ammonium hydroxide solution cooled in an ice bath. The slurry from both fractions was combined and allowed to precipitate for one day. The slurry was filtered and allowed to air dry. The fine powder was dissolved in 70-100 mL of ethanol and filtered and the precipitate was allowed to air dry. The powder was dissolved in methylene chloride and chromatographed on silica gel using ethyl acetate and ethyl alcohol in the ratio 50:50 as the eluent. The first band that came off the column was 5,15-(4-pyridyl)-10,20-(pentafluorophenyl)porphyrin. The second band was 5,10-(4-pyridyl)-15,20-(pentafluorophenyl)porphyrin. The third band that came off the column was tri-pyrido mono-pentafluorophenyl

porphyrin. The second band which was the desired band was collected and the solvent was removed by allowing it to evaporate. The product yield was 57.0 mg. (0.070 mmoles, 0.47% yield).  $R_f$  (ethyl acetate/ethanol 50:50) = 0.61.

UV-Vis ( $\text{CH}_3\text{CN}$ )  $\lambda_{\text{max}}$  (nm) [ $\epsilon \times 10^{-4}$  ( $\text{M}^{-1} \text{cm}^{-1}$ )] 410 [18.9], 507 [1.5], 581 [0.62], 648 [0.26].  $^1\text{H}$  NMR (300 MHz,  $\text{CDCl}_3$ , TMS):  $\delta$  9.09 (4H, dd, 2,6-pyridyl), 8.90 (4H, d, pyrrole), 8.86 (4H, d, pyrrole), 8.20 (4H, dd, 3,5-pyridyl), -2.92 (2H, s, internal pyrrole). [ $\text{C}_{42}\text{H}_{18}\text{N}_6\text{F}_{10} \cdot 1\text{C}_2\text{H}_5\text{OH}$ ] Anal Calcd (%): C, 62.71; H, 2.87; N, 9.97; Found: C, 62.54; H, 3.05; N, 9.86%. TOF-MS ES+( $m/z$ ; relative abundance): [ $\text{C}_{42}\text{H}_{17}\text{N}_6\text{F}_{10}$ ] $^+$  (796; 100).

[5,10-(4-pyridyl)-15,20-(pentafluorophenyl)porphyrin  $\text{Ru}_2(\text{bipy})_4\text{Cl}_2(\text{PF}_6)_2$  [*Cis*- $\text{H}_2(\text{DPyFP})\text{Ru}_2(\text{bipy})_4\text{Cl}_2(\text{PF}_6)_2$

A solution of 0.050 g (0.063 mmoles) of *cis*-5,10-(4-pyridyl)-15,20-(pentafluorophenyl)porphyrin and 0.058 g (0.12 mmoles) of *cis*- $\text{Ru}(\text{bipy})_2\text{Cl}_2$  was heated at reflux under nitrogen in 5 mL of glacial acetic acid for 45 min. The glacial acetic acid was removed under reduced pressure and the residue was taken up in a minimum (5 mL) of methanol and heated at reflux for 45 min. The reaction mixture was added dropwise to 60 mL of an aqueous solution of saturated ammonium hexafluorophosphate. The precipitate was filtered and washed with water. The powder was taken up in a minimum (5 mL) of acetonitrile and flash precipitated by addition to 100 mL of diethyl ether with stirring. The product was filtered and dried. The product yield was 0.050 gm. (0.025 mmoles, 40% yield). UV-Vis ( $\text{CH}_3\text{CN}$ )  $\lambda_{\text{max}}$  (nm) [ $\epsilon \times 10^{-4}$  ( $\text{M}^{-1} \text{cm}^{-1}$ )] 294 [9.6], 411 [13.9], 507 [2.8], 583 [0.9]. [ $\text{C}_{82}\text{H}_{50}\text{N}_{14}\text{F}_{22}\text{Cl}_2\text{P}_2\text{Ru}_2 \cdot 4\text{H}_2\text{O}$ ] Anal Calcd

(%): C, 47.44; H, 2.71; N, 9.19; F, 20.03; Found: C, 47.30; H, 2.51; N, 9.37; F, 19.83%. TOF-MS ES+ (m/z; relative abundance):  $[C_{82}H_{50}N_{14}F_{22}Cl_2P_2Ru_2]^+$  (1839; 46).

## DNA INTERACTIONS

### Materials:

Electrophoresis-grade low EEO agarose, tris(hydroxymethyl)-aminoethane (Tris), sodium chloride, and boric acid were obtained from Fisher. The plasmid, pUC18, was obtained from Bayou Biolabs. Ethidium bromide was obtained from EM. Agarose gel 6X loading dye was used to prepare the samples for loading on gel. The spectroscopic titration was carried out at room temperature in the buffer (5 mM Tris, 0.1 M NaCl, pH 7.16). Concentration of the calf thymus (CT) DNA (Sigma) solution used in titrations was determined spectrophotometrically using the extinction coefficient  $6600 \text{ M}^{-1}\text{cm}^{-1}$  at 260 nm.<sup>47</sup> All aqueous solutions were prepared using doubly distilled water. APEX illuminator (Oriel Inst., New port) was used to irradiate the samples. Electronic UV transilluminator (ULTRA. LUM. INC) was used for viewing DNA in agarose gels stained with ethidium bromide. Incubator (Barnstead labline) was used to incubate the samples in the experiments which were run in the dark. The pH of the solutions was measured using a Denver instruments pH meter.



### **DNA binding titrations**

Preparation of buffer (5 mM Tris, 0.1 M NaCl): 0.0610 g of tris(hydroxymethyl)-aminoethane (Tris) and 0.584 g of sodium chloride were weighed and dissolved in 100 mL of deionized water. The pH of the buffer was measured to be 7.16.

CT DNA was dissolved in buffer and the concentration of this solution was determined spectrophotometrically using the extinction coefficient  $6600 \text{ M}^{-1}\text{cm}^{-1}$  at 260 nm giving a concentration of 330  $\mu\text{M}$ .

A stock solution of ruthenium porphyrin (II) (19.5  $\mu\text{M}$ ) in 10% DMSO /H<sub>2</sub>O was diluted to 9.75  $\mu\text{M}$  using the Tris buffer solution. For DNA titrations 3.5 mL of the diluted ruthenium porphyrin was placed in a 1 cm quartz cuvette. Aliquots (10  $\mu\text{L}$ ) of the CT-DNA solution were added to the cuvette and the Soret band associated with the ruthenium porphyrin (II) was monitored. Additions were made until the spectra did not change or the solution became turbid.

### **Photocleavage of circular plasmid DNA:**

The 5X TB buffer used for electrophoresis was prepared by dissolving 27.5 g Boric acid and 54.0 g Tris base in 1 L volumetric flask with deionized water.

Preparation of agarose gel:

To 0.8 g of agarose weighed accurately, 80 mL of doubly distilled water was added and heated in a microwave for 2.5 min on low power. 20 mL of 5X TB buffer was added and swirled to mix well and then this liquid agarose solution was poured into the gel rig tray. An appropriate size comb was inserted into the liquid agarose and the gel was allowed to solidify. Once the gel solidified the buffer solution was added. The buffer was prepared by obtaining 150 mL of 5X

TB buffer and diluting to 600 mL with doubly distilled water and then poured over the solidified gel.

Preparation of the metal complex:

10.1  $\mu$ M ruthenium porphyrin (II) in 10 % DMSO was prepared and used for photocleavage studies.

Two solutions were prepared in 1.5 mL eppendorf tubes which includes one for control (DNA with no metal complex added) and other for the test (DNA with metal complex). 5  $\mu$ L of 1  $\mu$ g/1 $\mu$ L pUC 18 DNA was added to both tubes. An appropriate amount of metal complex solution was added to the test solution to give the desired 5 DNA BP:metal complex ratio. An appropriate amount of doubly distilled water was added to both tubes to bring the final volume to 500  $\mu$ L. Both tubes were vortexed and then spun in a centrifuge for 30 seconds. The control and test solutions were transferred to quartz cuvettes and placed side by side and irradiated with a 50 W tungsten halogen lamp from an APEX illuminator. At 0, 30, 60, 90 and 120 minute time intervals 20  $\mu$ L aliquots were pipetted into the eppendorf tubes. 4  $\mu$ L of 6X loading dye was pipetted into each tube and all the 10 tubes were vortexed and spinned in the centrifuge. The samples were then loaded onto the agarose gel and subjected to 150 V voltage for 1 hour. The gel was then soaked in ethidium bromide staining solution for 1 hour. The ethidium bromide staining solution was prepared by adding 30  $\mu$ L of ethidium bromide to 250 mL of deionized water and mixing well. The gel was then photographed using UV illumination.

To reveal the importance of light, experiments were run in the absence and presence of light and a comparison was made. In this study two sets of solutions were prepared. Each set consists of a control and a test solution. 5  $\mu\text{L}$  of pUC 18 DNA was added to both control and test solution. An appropriate amount of metal complex solution was added to the test solution to give the desired 5 DNA BP:metal complex ratio. Appropriate amount of doubly distilled water was added to both control and test solutions to bring the final volume to 500  $\mu\text{L}$ . Then one set of solutions was placed in an incubator at 37°C for 2 hours and the other set was irradiated for 2 hours with a 50 W tungsten halogen lamp from an APEX illuminator. The samples were loaded onto agarose gel and subjected to an electric field by applying 150 V voltage for 1 hour. The gel was then soaked in ethidium bromide staining solution for 1 hour and photographed using UV illumination.

## CHAPTER 3

### RESULTS AND DISCUSSION

#### Synthesis and characterization

The *cis*-porphyrin (I) was synthesized by reaction of pentafluorobenzaldehyde, 4-pyridinecarboxaldehyde and pyrrole in the stoichiometric ratio 1:3:4 respectively in refluxing propionic acid, Figure 13.

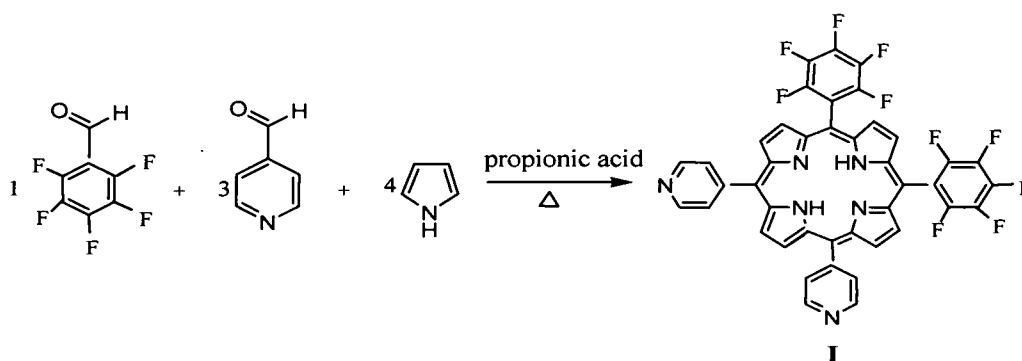


**Figure 13:** Synthesis of 5,10-(4-pyridyl)-15,20-(pentafluorophenyl)porphyrin.

The major product of this reaction is the polymeric material while the minor product is the formation of *cis*-porphyrin (I) along with five other porphyrins, Figure 14. Attempts to increase the yield of the *cis*-porphyrin (I) by varying the ratio of the aldehydes led to the ratio shown in Figure 13 which indicates that pentafluorobenzaldehyde is more reactive than 4-pyridine carboxaldehyde. The polymeric byproducts were removed by washing with ethanol.

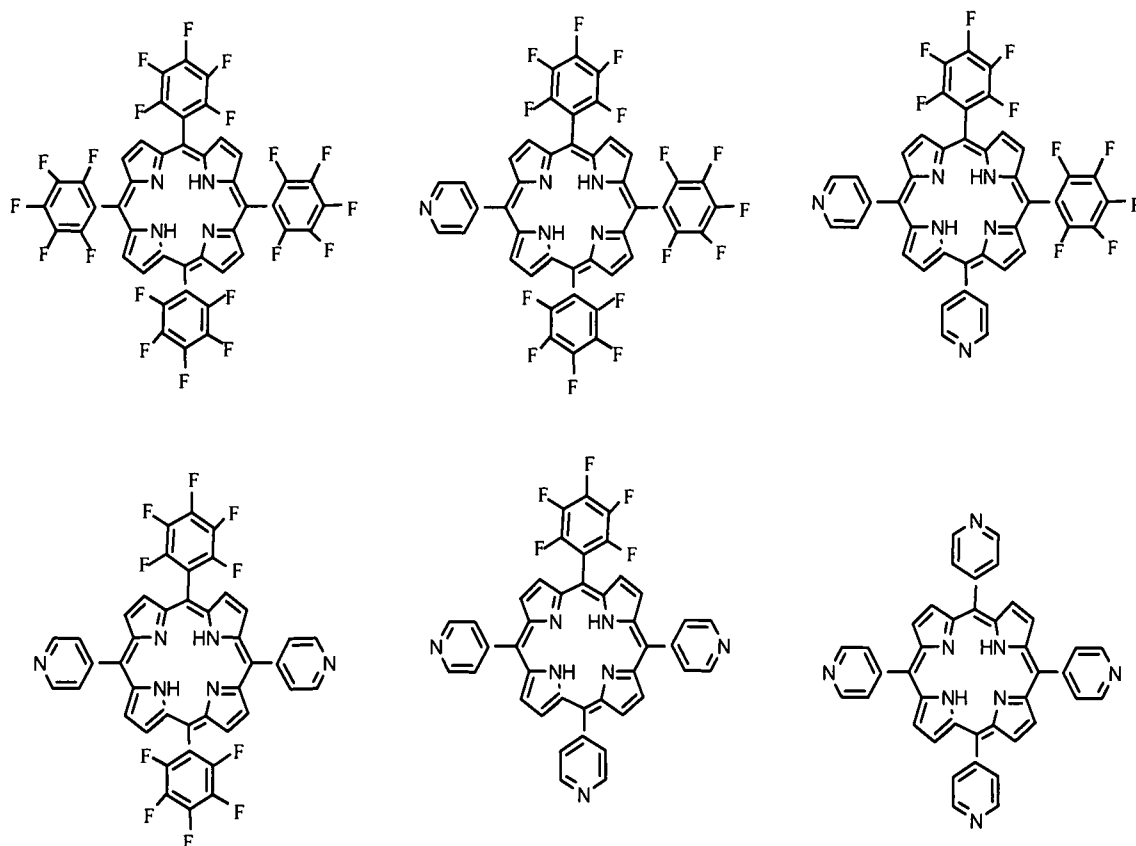


**Figure 14:** Six different porphyrins resulted by reacting two different aldehydes with pyrrole in propionic acid.

Separation of the remaining six porphyrins was accomplished by column chromatography. Previous attempts to separate the six porphyrins by chromatographic separation using methylene chloride:acetone as the eluent were not successful in separating the *cis/trans* isomers. Hence different solvent systems were employed to achieve the separation of the *cis*-porphyrin (I). The crude product was dissolved in a minimal amount (ca 20 mL) of methylene chloride and filtered to remove insoluble materials. The product solution was carefully added to the column and eluted with 50:50 ethyl acetate:ethanol which

resulted in the clean separation of the *cis*- porphyrin (I) as the second band. The yield of the product was very low and reported to be 0.47%. Thin layer chromatography was performed to determine the retention factor  $R_f$  for the *cis* porphyrin (I). The *cis*-porphyrin (I) being more polar than the *trans* isomer possess lower  $R_f$  value (0.61) when compared to the *trans*-porphyrin (0.83) which was separated as the first band during the chromatographic separation. The mono-pyridyl tri-pentafluorophenyl porphyrin was washed along with the polymer and the tri-pyridyl mono-pentafluorophenyl porphyrin was separated as the third band. The *cis*- porphyrin (I) was characterized by  $^1\text{H}$  NMR, high resolution mass spectroscopy and elemental analysis.

Ruthenium porphyrin (II) was synthesized by adding the *cis*-porphyrin (I) to *cis*- $\text{Ru}(\text{bipy})_2\text{Cl}_2$  in a stoichiometric ratio 1:2 and refluxing in glacial acetic acid, Figure15.

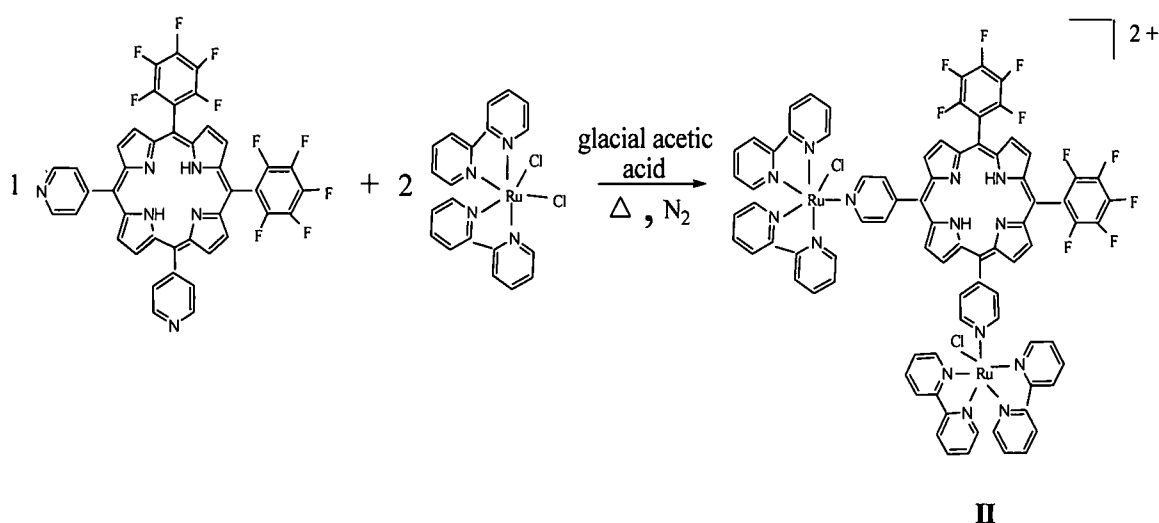


**Figure 15:** Synthesis of [5,10-(4-pyridyl)-15,20-(pentafluorophenyl)porphyrin- $\text{Ru}_2(\text{bipy})_4\text{Cl}_2$ ] $^{2+}$

Substitution of the ruthenium polypyridyl complex to the peripheral pyridyl of the porphyrin involves displacement of a chloride ion from the sixth position. Since six coordinate Ru(II) complexes are typically substitution inert, extreme conditions like refluxing in glacial acetic acid are required. After the acetic acid is removed under reduced pressure the resulting reaction mixture is refluxed and precipitated from methanol by addition of ammonium hexafluorophosphate. The product was isolated in descent yields and was characterized by high resolution mass spectroscopy and elemental analysis.

#### **Electronic absorption spectroscopy:**

The UV-Vis studies of the *cis*-porphyrin (I) and its ruthenated analog (II) were run in 1 cm quartz cuvettes in acetonitrile at room temperature. The UV-Visible absorption spectrum of a typical porphyrin exhibits an intense absorption at about 400 nm (the Soret band) followed by several weaker absorptions (Q bands) at higher wave lengths from 450 to 700 nm. Comparision of the electronic transitions of *cis*-porphyrin (I) and its ruthenated analog (II) is illustrated in the Figure 16. The *cis*-porphyrin (I) (red line, Figure 16) shows an intense absorption at 410 nm for the Soret band and three less intense Q bands at the wavelengths 506, 581 and 648 nm. The highest energy electronic absorption at 294 nm for the ruthenium porphyrin (II) is assigned as a bipy ( $\pi$ -  $\pi^*$ ) intraligand charge transfer. Two shoulders at ca. 360 and 470 nm are attributed to Ru( $d\pi$ ) - bipy( $\pi^*$ ) metal to ligand charge transfer (MLCT) transition. The details of these transitions and the molar absorptivities of the Soret and Q bands of *cis* porphyrin (I) and ruthenium porphyrin (II) are illustrated in Table 1.

The electronic spectra of ruthenium porphyrin is an overlay of ruthenium spectra and porphyrin spectra separately. This indicates that there is very little electronic communication between ruthenium and porphyrin which would otherwise cause a shift in the Soret band.

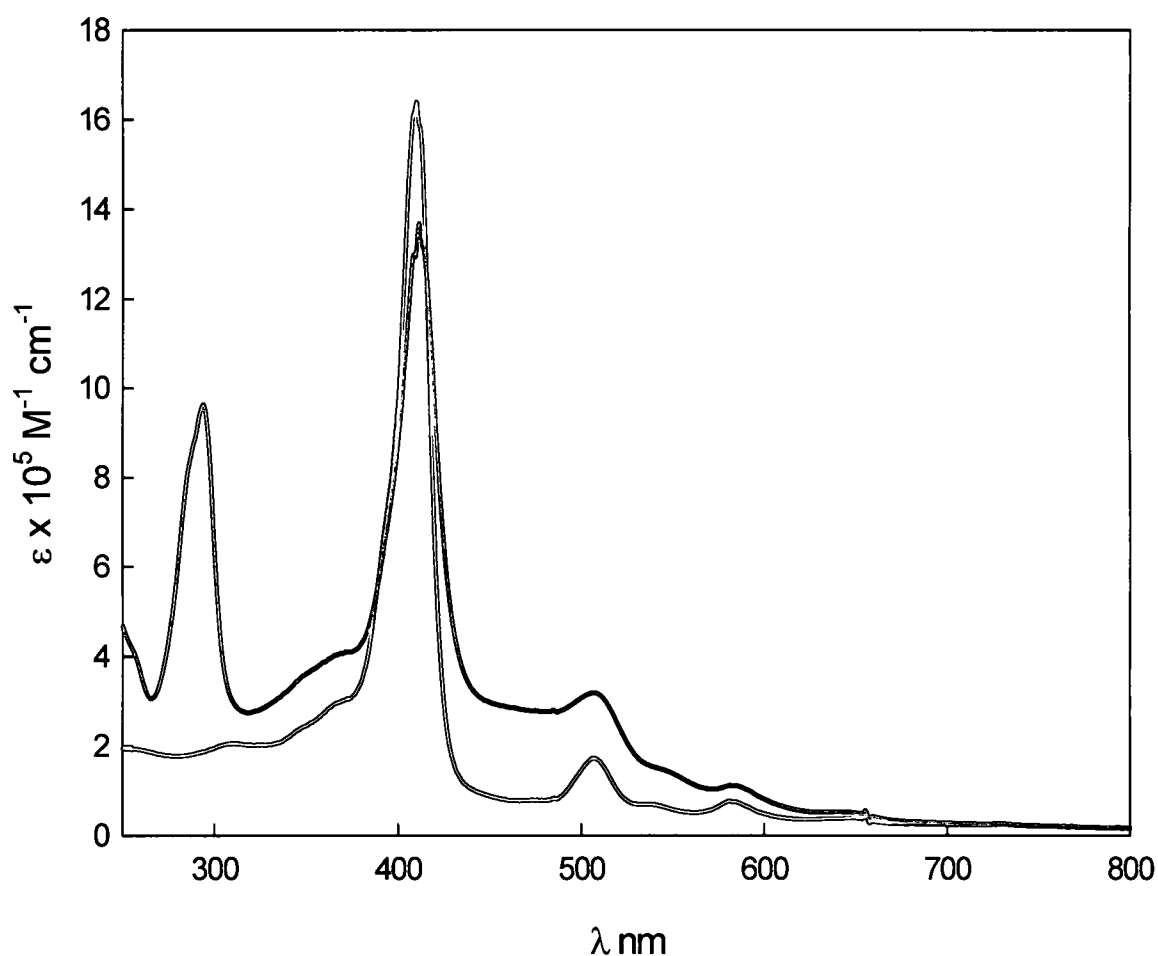


**Figure 16:** Electronic absorption spectra in acetonitrile at room temperature for *cis* porphyrin (I) (red) and ruthenium porphyrin (II) (blue).



**Table 1:** Electronic absorption spectroscopy results for *cis* porphyrin (I) and ruthenium porphyrin (II).

Complex	$\lambda_{\max}$ (nm)	$\epsilon \times 10^{-4} \text{ M}^{-1} \text{ cm}^{-1}$	Assignment
<b><i>cis</i> porphyrin</b>	410	18.9	Soret ( $\pi - \pi^*$ )
	506	1.5	Q band
	581	0.62	Q band
	648	0.26	Q band
<b>Ruthenium porphyrin</b>	294	9.6	bipy( $\pi$ ) – bipy( $\pi^*$ )
	360	sh	Ru( $d\pi$ ) - bipy( $\pi^*$ )
	411	13.9	Soret ( $\pi - \pi^*$ )
	470	sh	Ru( $d\pi$ ) - bipy( $\pi^*$ )
	507	2.8	Q band
	583	0.9	Q band

### Solution Electrochemistry

Solution phase cyclic voltammetry (CV) was performed using a one compartment, three electrode cell, equipped with a platinum wire auxiliary electrode. The working electrode was a 2.0 mm diameter glassy carbon electrode. Potentials were referenced to a Ag/AgCl electrode. The supporting electrolyte was 0.1 M tetrabutyl ammonium hexafluorophosphate (TBAPF<sub>6</sub>) and the measurements were made in extra dry, < 50 ppm water, acetonitrile, purged with N<sub>2</sub> to remove oxygen from the solution. The cyclic voltammograms of the *cis* porphyrin (I) and its ruthenium analog (II) are illustrated in Figure 17.

When the *cis*- porphyrin (I) solution is cycled in the cathodic direction two quasireversible redox couples with  $E_{1/2} = -0.86 \text{ V}$  and  $-1.26 \text{ V}$  versus Ag/AgCl are observed. These redox couples can be associated with sequential reduction of the porphyrin ring to form the radical anion. In the anodic direction there is a

weak irreversible oxidation process at  $E_{pa} = 1.15$  V versus Ag/AgCl due to the porphyrin oxidation, Figure 17 (red line). Table 2 illustrates the redox potentials and their assignments.

When the ruthenium porphyrin (II) solution is cycled in the cathodic direction two quasireversible redox couples with  $E_{1/2} = -0.80$  and  $-1.18$  V versus Ag/AgCl are observed which are attributed to a porphyrin centered redox process. In the anodic direction, a quasireversible redox couple with  $E_{1/2} = 0.83$  V versus Ag/AgCl associated with the  $Ru^{(III/II)}$  couple is observed, Figure 17 (blue line). The redox potentials in the cathodic region for ruthenium porphyrin (II) and *cis*-porphyrin (I) are very similar to each other. This indicates the fact that there is very little electronic communication between ruthenium and porphyrin which would otherwise cause a greater difference in the redox potentials in the cathodic region than what is observed.

**Table 2:** Redox potentials and their assignments for *cis* porphyrin (I) and ruthenium porphyrin (II).

Complex	$E_{1/2}$ (V)	Assignment
Cis-porphyrin	-0.86	Por <sup>0/-</sup>
	-1.26	Por <sup>-2-</sup>
Ruthenium porphyrin	0.83	$Ru^{(III/II)}$
	-0.80	Por <sup>0/-</sup>
	-1.18	Por <sup>-2-</sup>

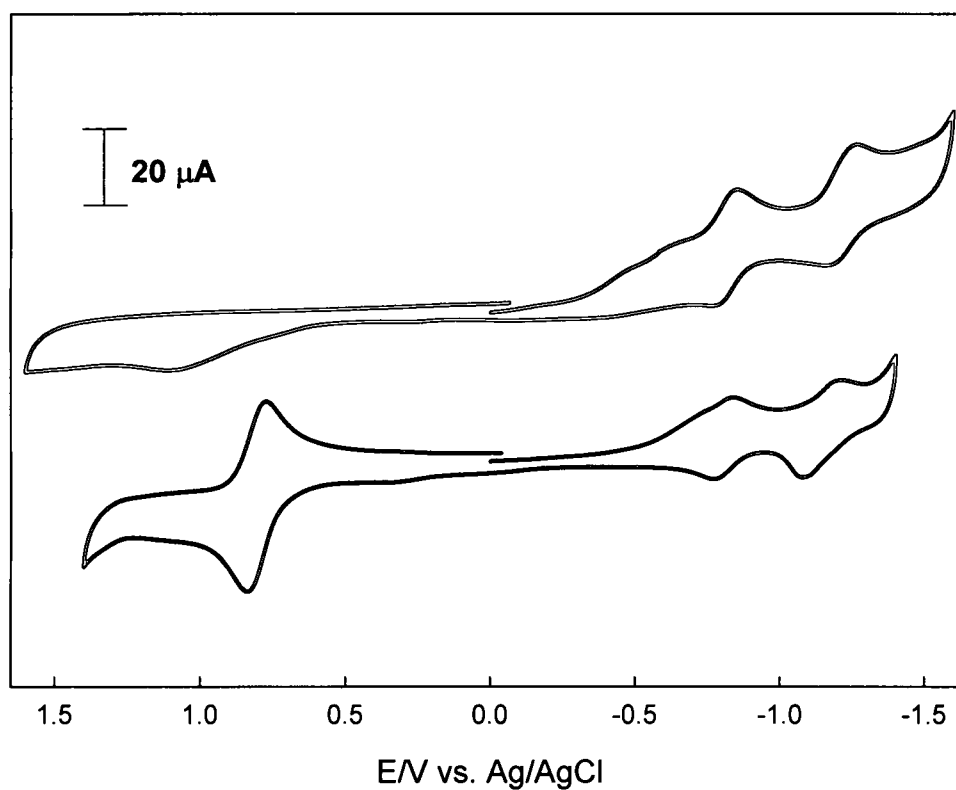
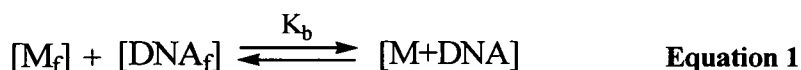


**Figure 17:** Cyclic voltammograms of *cis* porphyrin (I) (red) and ruthenium porphyrin (II) (blue) in  $\text{TBAPF}_6/\text{Acetonitrile}$  vs  $\text{Ag}/\text{AgCl}$ . Working electrode is glassy carbon with a scan rate of 100  $\text{mV}/\text{s}$ ,  $\text{N}_2$  atmosphere.

## CHAPTER 4

### DNA INTERACTIONS

There are several ways in which complexes can interact with DNA. Complexes can interact with DNA by covalently binding, electrostatically binding, groove binding or by intercalating. Studies on several compounds of ruthenium like  $[\text{Ru}(\text{bpy})_2\text{L}]^{2+}$  and  $[\text{Ru}(\text{phen})_2\text{L}]^{2+}$  where L is an aromatic bidentate ligand, indicate that these compounds bind to DNA, often in an intercalative fashion.<sup>48</sup> DNA binding constants,  $K_b$  are the most commonly used measures of DNA binding affinity. The association of metal complex with DNA is treated as a simple equilibrium, as shown in equation 1, where  $M_f$  is the free complex (in this case, ruthenium porphyrin),  $\text{DNA}_f$  is free DNA, and MDNA is a bound ligand and bound binding site.



To determine quantitatively a binding constant ( $K_b$ ) for the interaction of ruthenium porphyrin (II) with DNA, absorption titrations were used. Aqueous solutions of ruthenium porphyrin (II) which were 5% in DMSO were titrated with pH 7.16 buffered solutions (5 mM Tris, 0.1 M NaCl) of calf thymus (CT) DNA. The concentration of the ruthenium porphyrin (II) was 9.75  $\mu\text{M}$  and the concentration of CT-DNA was 330  $\mu\text{M}$ . 5 mM Tris, 0.1 M NaCl was used as the

buffer solution. An aliquot of 10  $\mu\text{L}$  DNA was added to the ruthenium porphyrin (II) and the absorbance of the Soret band was recorded. Figure 18 illustrates the effects of additions of 10  $\mu\text{L}$  aliquots of CT-DNA on the absorbance of the Soret band associated with ruthenium porphyrin (II). As the concentration of CT-DNA increases the Soret band decreases and shifts to lower energy (415-423 nm). This red shift is indicative of intercalative binding to DNA.<sup>49</sup>

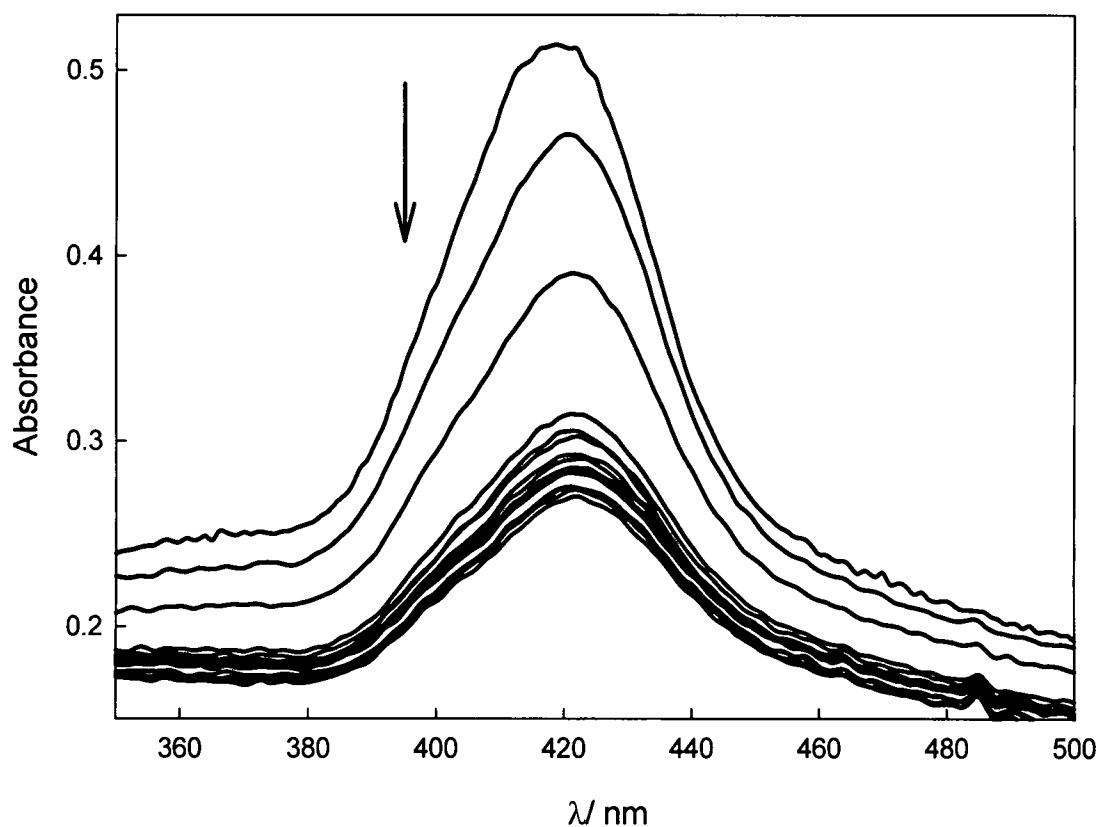


**Figure 18:** Absorption spectra of pH 7.16 buffer solutions of ruthenium porphyrin (II) in the presence of increasing amounts of CT-DNA. [ruthenium porphyrin (II)] = 9.75  $\mu\text{M}$ .

The intrinsic binding constant  $K_b$  for the CT-DNA ruthenium porphyrin interaction was determined from equation 2.<sup>50</sup>

$$[\text{DNA}] / (\epsilon_a - \epsilon_f) = [\text{DNA}] / (\epsilon_b - \epsilon_f) + 1/K_b(\epsilon_b - \epsilon_f) \quad \text{Equation 2}$$

where  $\epsilon_a$  = absorbance/ [ruthenium porphyrin],  $\epsilon_b$  and  $\epsilon_f$  are the extinction coefficients for the fully bound form and the extinction coefficient for the free form of ruthenium porphyrin(II), respectively. A linear fit of the plot of  $[\text{DNA}] / (\epsilon_a - \epsilon_f)$  versus  $[\text{DNA}]$  gives a slope of  $1/(\epsilon_b - \epsilon_f)$  and an intercept of  $1/ K_b(\epsilon_b - \epsilon_f)$ , Figure 19. The intrinsic binding constant  $K_b$  is given by the ratio of the slope to intercept.

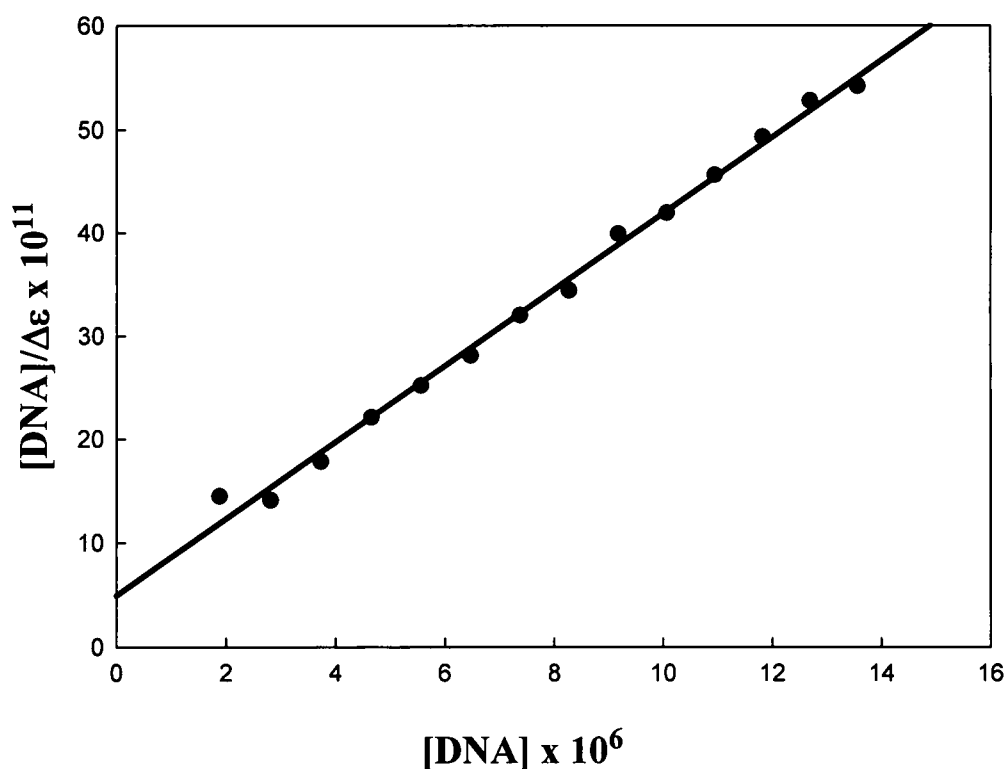


**Figure 19:** Plot of  $[\text{DNA}]/(\epsilon_a - \epsilon_f)$  versus  $[\text{DNA}]$

This half-reciprocal absorption titration method, which has been used successfully to determine the intrinsic  $K_b$  of molecules as hydrophobic as benzo pyrene derivatives, was found to provide a useful route to obtain intrinsic binding constant for the broad range of ruthenium complexes of different solubilities.<sup>51</sup> A value of  $7.6 \times 10^5 \text{ M}^{-1}$  was determined for ruthenium porphyrin (II) by this method. A value of  $2.0 \times 10^4 \text{ M}^{-1}$  was determined for the *cis* porphyrin (I) by this method. The magnitude of  $K_b$  coupled with the red shift of the Soret band suggests an intercalative process for the binding of ruthenium porphyrin (II) with DNA.<sup>49</sup> The greater binding constant for ruthenium porphyrin (II) compared to *cis* porphyrin (I) is most likely due to the increased charge of the complex and therefore is an effect of increased electrostatic attraction.

### **Photocleavage of circular plasmid DNA**

Agarose gel electrophoresis was performed to determine the photocleavage of circular plasmid DNA by ruthenium porphyrin (II). Gel electrophoresis is a method for separating chemical compounds based on their size, shape and charge. Gel electrophoresis is used to identify distinct conformations of circular plasmid DNA. Supercoiled DNA (Form I), is the fastest moving conformation in the gel because of its compact shape. Nicked circular DNA (Form II) is also called relaxed circle and it is the slowest conformation of circular plasmid in the gel. In the nicked circular DNA, the superhelical tension relaxes and the tightly wound ball becomes a floppy circle. In electrophoresis experiments the DNA fragments are injected into the wells in solidified agarose

gel and subjected to an electric field. Since the DNA is negatively charged the fragments that are loaded into a sample well at the cathode (-) end of a gel move through the gel towards the anode (+). The mobility of DNA fragments on the gel is dependent on the size, shape and the overall charge.

The DNA gels are made of agarose, a highly purified agar, which is heated and dissolved in a buffer solution. The agarose molecules form a matrix with pores. Agarose gels can be used to analyze double-stranded DNA fragments from 70-base-pairs (bp) (3% agarose gel, w/v) to 800,000 bp (0.1% agarose gel).<sup>52</sup> In this project 0.8% agarose gel is used.

The solutions of circular plasmid DNA with and without ruthenium porphyrin (II) were placed in two different quartz cuvettes and irradiated with a 50 W quartz tungsten halogen lamp for 120 minutes. At 30 min intervals aliquots of both solutions were removed and prepared for gel electrophoresis. Figure 20 illustrates the results of the gel electrophoresis study.



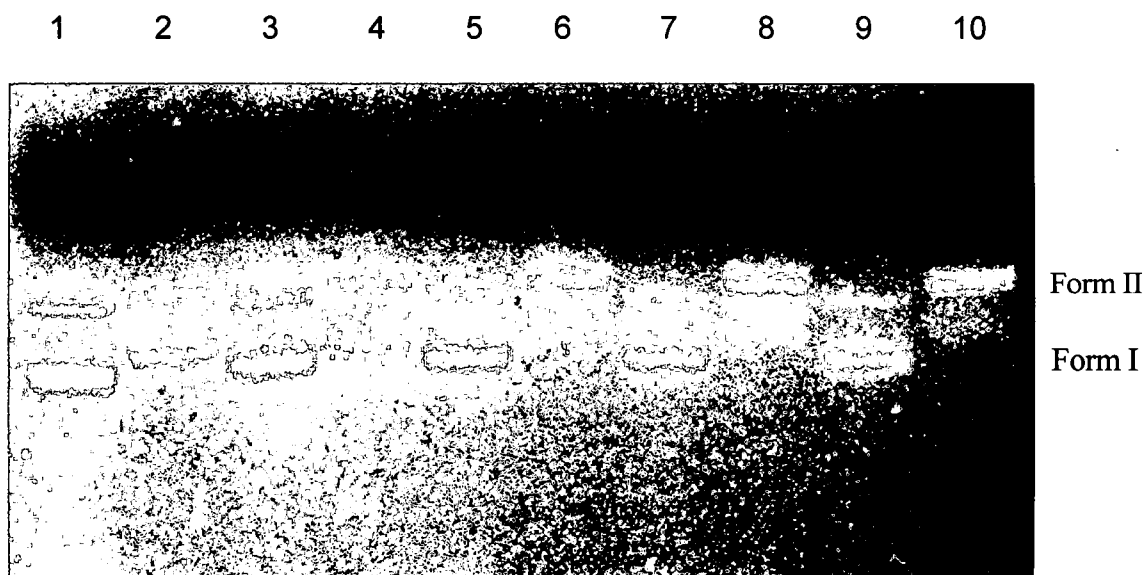


**Figure 20:** Gel electrophoresis results of circular plasmid DNA (pUC18) in the presence of ruthenium porphyrin (lanes 2, 4, 6, 8, 10) and without ruthenium porphyrin (lanes 1, 3, 5, 7, 9) irradiated with 50 W quartz tungsten halogen lamp for 0 min (lanes 1 and 2), 30 min (lanes 3 and 4), 60 min (lanes 5 and 6), 90 min (lanes 7 and 8) and 120 min (lanes 9 and 10).

When buffered solutions of circular plasmid DNA (pUC18) containing ruthenium porphyrin (II) in a ratio of 5:1 bp:ruthenium porphyrin, are irradiated with light the supercoiled DNA (Form I) is converted to nicked circular DNA (Form II). Lanes 1, 3, 5, 7 and 9 represent buffered solutions of pUC18 without ruthenium porphyrin (II) irradiated for 0, 30, 60, 90 and 120 min, respectively. Lanes 2, 4, 6, 8 and 10 represent buffered solutions of pUC 18 with ruthenium porphyrin (II) irradiated for 0, 30, 60, 90 and 120 min, respectively. Lanes 2, 4, 6, 8 and 10 illustrate a decrease of form I and an increase of form II. As the irradiation time increases the circular DNA has been converted to nicked DNA. After 2 hours of irradiation the plasmid DNA without ruthenium porphyrin (lane 9)

remains unchanged while the circular plasmid DNA in the presence of ruthenium porphyrin (II) (lane10) has been completely converted to the nicked form (Form II). Hence gel electrophoresis results suggests that the ruthenium porphyrin (II) can photolytically cleave circular DNA.

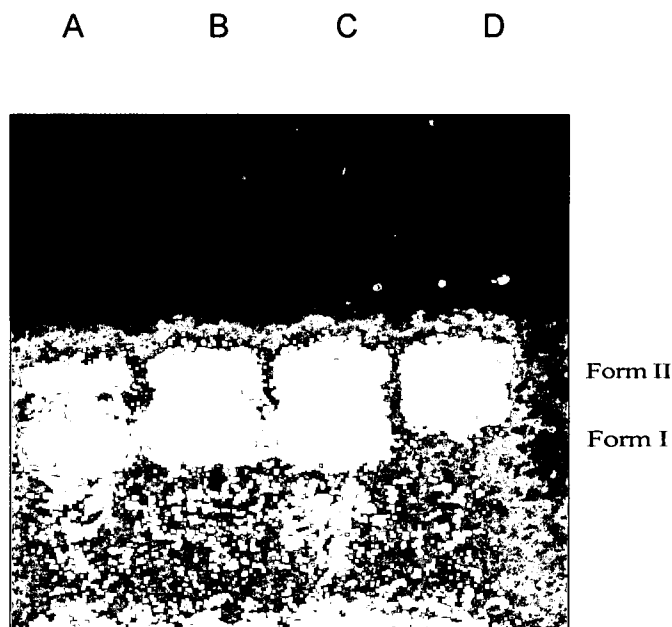


**Figure 21:** Gel electrophoresis results both in the absence and presence of light. Lanes A and B represent the circular plasmid DNA (pUC18) in the absence and presence of ruthenium porphyrin respectively incubated for 2 hours at 37°C. Lanes C and D represent the circular plasmid DNA (pUC18) in the absence and presence of ruthenium porphyrin respectively irradiated with light for 2 hours.

To show that photocleavage of DNA requires both the ruthenium porphyrin and light, experiments were run in which solutions of pUC18 with and without ruthenium porphyrin (II) were irradiated for 2 hours. Simultaneously the same solutions were incubated in the dark for 2 hours followed by gel electrophoresis, Figure 21. Lanes A and B represent the circular plasmid DNA (pUC18) in the absence and presence of ruthenium porphyrin (II) (5:1 bp:metal complex ratio)

respectively, incubated for 2 hours at 37°C. Lanes C and D represent the circular plasmid DNA (pUC18) in the absence and presence of ruthenium porphyrin (II) (5:1 bp:metal complex ratio) respectively irradiated with 50 W quartz tungsten halogen lamp for 2 hours. Lanes A ,B and C reveal no difference in the plasmid DNA where as in lane D the circular plasmid DNA has been converted to the nicked form (Form II). Hence the results reveal that the process is light induced.

## CHAPTER 5

### CONCLUSIONS

This study describes the synthesis of two new complexes, 5,10-(4-pyridyl)-15,20-(pentafluorophenyl)porphyrin (I) and 5,10-(4-pyridyl)-15,20-(pentafluorophenyl)porphyrin  $\text{Ru}_2(\text{bipy})_4\text{Cl}_2$  (II) and characterization of these complexes by UV-Vis spectroscopy, solution electrochemistry,  $^1\text{H}$  NMR, elemental analysis and high resolution mass spectroscopy. The intrinsic binding constant ( $K_b$ ) for these complexes was determined by Spectroscopic titrations with calf thymus DNA. A value of  $7.6 \times 10^5 \text{ M}^{-1}$  was determined for the ruthenium porphyrin (II) and a value of  $2.0 \times 10^4 \text{ M}^{-1}$  was determined for the *cis* porphyrin (I). The magnitude of  $K_b$  coupled with the red shift of the Soret band suggests an intercalative process for the binding of these complexes with DNA. Agarose gel electrophoresis was performed to determine the photocleavage of circular plasmid DNA by ruthenium porphyrin (II) and the results reveal that the ruthenium porphyrin (II) can photolytically cleave circular DNA.

## CHAPTER 6

### FUTURE EXPERIMENTS

The present studies reveal that the ruthenium porphyrin (II) can photolytically cleave circular DNA. Further studies are underway to synthesize a tri-pyrido mono pentafluorophenyl ruthenated porphyrin and determine its photolytic cleavage of circular plasmid DNA. The proposed structure of porphyrin for future studies is illustrated in Figure 22.

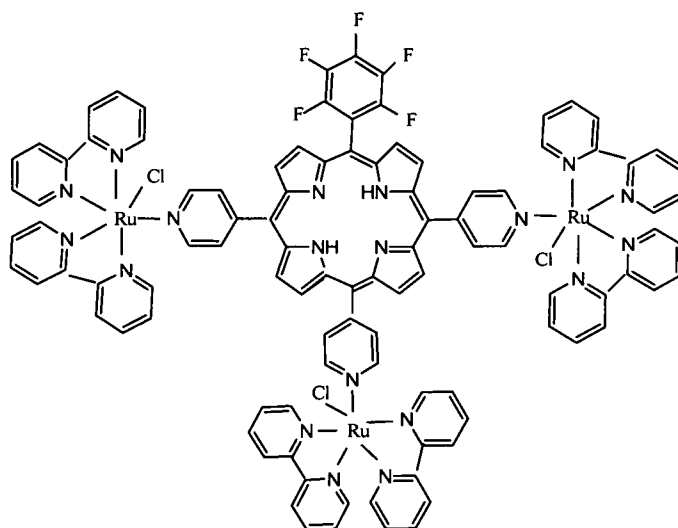


**Figure 22:** Proposed structure of porphyrin for future study.

## CHAPTER 7

### BIBLIOGRAPHY

1. Henderson, B.W.; Dougherty, T.J. *Photodynamic therapy: Basic Principles and Clinical applications*, Marcel Dekker: New York, **1992**.
2. Raab, O.Z. *Biol.* **1900**, 39, 524.
3. Von Tappeiner, H.; Jesionek, A. *Muench.Med.Wochschr.* **1903**, 47, 2042.
4. Meyer-Bertz, F. *Dtsch. Arch. Klin. Med.* **1913**, 112, 476.
5. Policard, A.C. *R. Soc. Biol.* **1924**, 91, 1423.
6. Von Tappeiner, H.; Jadbauer, A. *Dtsch. Arch. Klin. Med.* **1904**, 80, 427.
7. Sternberg, E.D.; Dolphin, D.; Bruckner, C. *Tetrahedron.* **1998**, 54, 4151.
8. Macdonald, I.J.; Dougherty, T.J. *J.Porphyrins pthalocyanines.* **2001**, 5, 105.
9. Alan, R.; Liss CSF. *Mechanisms of Photo-oxygenation*. New York: **1984**.
10. Chen, M.; Pennathur, A.; Luketich, J.D. *Role of Photodynamic therapy in Unresectable Esophageal and lung cancer. Lasers Surg Med.* **2006**, 38, 396-402.
11. Pandey, R.K.; Bellnier, D.A.; Smith, K.M, etal. *Chlorin and Porphyrin derivatives as Potential photosensitizers in Photodynamic Therapy. Photochemistry and Photobiology.* **1991**, 53, 65-72.
12. Dougherty, T.J.; Gomer, C.J.; Henderson, B.W, etal. *Photodynamic Therapy. Journal of the National Cancer Institute.* **1998**, 90, 889-905.
13. Dashwood, R. H. *Int. J. Oncol.* **1997**, 10, 721.

14. Grosjean, P.; Savary, J.; Wagnieras, G. *Laser Med. Sci.* **1993**, *8*, 235.
15. Patrice, T. *Int. Photodyn.* **1995**, *1*(3), 1-2.
16. Levy, J.G.; Jones, C.A. and Pilson, L.A. *Int. Photodyn.* **1994**, *1*(1), 3-5.
17. Hunt, D.W.C.; Chan, A.H. and Levy, J.G. *Int. Photodyn.* **1998**, *1*(3), 2-4.
18. Stables, G.I. and Ash, D.V. *Cancer Treat. Rev.* **1995**, *21*, 311-323.
19. (a) Ali, H.; van Lier, J.E. *Chem. Rev.* **1999**, *99*, 2379. (b) Nyman, E.S.; Hynninen, P.H. *J. Photochem. Photobiol, B: Biol.* **2004**, *73*, 1.
20. van Lier, J.E. and Spikes, J.D. The chemistry, photophysics and photosensitizing properties of Pthalocyanines, eds. G. Bock and S. Harnett, pp. 17-32 (John Wiley & Sons Ltd, Chichester. UK., **1989**)
21. Kennedy, J.C.; Pottier, R.H. Endogenous Protoporphyrin IX, a clinically useful Photosensitizer for Photodynamic therapy. *J Photochem Photobiol B.* **1992**, *14*, 275-92.
22. Lipson, R. L.; Baldes, E. J.; Gray, M. J. *Cancer.* **1967**, *20*, 2255-2257.
23. Nencki, M and Sieber, N., *Arch. Explt. Path. Pharmacol.* **1884**, *18*, 401.
24. Kuster, W.Z., *Z. Physiol. Chem.* **1912**, *82*, 463.
25. Dougherty, T.J.; Grindley, G.E.; Fiel, R., etal. *J Natl Cancer Inst.* **1975**, *55*, 115-121.
26. Yang, S.I.; Seth, J.; Strachan, J.P.; Gentemann, S.; Kim, D.; Holten, D.; Lindsey, J.S.; Bocian, D.F. *J. Porph. Phthal.* **1999**, *3*, 117.
27. Chen X.; Hui L.; Foster, D.A.; Drain, C.M. *Biochemistry.* **2004**, *43*, 10918.
28. Fu, P. K.L. ; Bradley, P.M.; van Loyen, D.; Dyrr, H.; Bossmann, S.H.; Turro, C. *Inorg. Chem.* **2002**, *41*, 3808.

29. Lecomte, J.-P.; Kirsch-De Mesmaeker, A.; Feeney, M.M.; J.M. Inorg. Chem. **1995**, *34*, 6481.
30. Pogozelski, W.K.; Tullius, T. D. Chem. Rev. **1998**, *98*, 1089.
31. Armitage, B. Chem. Rev. **1998**, *98*, 1171.
32. Erkkila, K. E.; Odom, D.T.; Barton, J.K. Chem Rev. **1999**, *99*, 2777.
33. Yam, V. W.-W.; Lo, K.K.-W.; Cheung, K.-K.; Kong, R. Y.- C. J. Chem. Soc. Dal. Trans. **1997**, *12*, 2067.
34. Sitlani, A.; Long, E. C.; Pyle, A.M.; Barton, J. K. J. Am. Chem. Soc. **1992**, *114*, 2303.
35. Bradley, P.M.; Angeles-Boza, A.M.; Dunbar, K.R.; Turro, C. Inorg. Chem. **2004**, *43*, 2450.
36. Swavey, S.; Brewer K. J. Inorg Chem. **2002**, *41*, 6196.
37. Claire, S. Allardyce.; Paul, J. Dyson. Ruthenium in medicine :Current Clinical Uses and Future Prospects.
38. Lerman, L.S. J. Mol. Biol. **1961**, *3*, 18.
39. Barton, J.K.; Raphael, A.L. Proc. Natl. Acad. Sci. U.S.A. **1985** , *82*, 6460.
40. Holmlin, R.E.; Stemp, E.D.A.; Barton, J.K. Inorg.Chem. **1998**, *37*, 29.
41. Friedman, A.E.; Chambron, J.C.; Sauvage, J.P.; Turro, N.J.; Barton, J.K. J. Am. Chem. Soc. **1990**, *112*, 4960.
42. Moucheron, C.; Kirschdemesmaeker, A.; Kelly, J.M. J. Photochem. Photobiol. B. **1997**, *40*, 91.
43. Carlson, D.L.; Huchital, D.H.; Mantilla, E.J.; Sheardy, R.D.; Murphy, W.R. J. Am. Chem. Soc. **1993**.



R002593549

44. Araki, K.; Toma H.E. *Inorg. Chim. Acta.* **1991**, *179*, 293.
45. Deng, H.; Li, J.; Zheng, K.C.; Yang, Y.; Chano, H.; Ji L.N. *Inorg. Chim. Acta.* **2005**, *358*, 3430.
46. Sullivan, B.P.; Salmon, D.J.; Meyer, T.J. *Inorg. Chem.* **1978**, *17*, 3334.
47. Reichmann, M.F.; Rice, S.A.; Thomas, C.A.; Doty, P. *J. Am. Chem. Soc.* **1954**, *76*, 3047.
48. Gao, F.; Chao, H.; Zhou, F.; Yuan, Y. X.; Peng, B.; Ji, L. N., J. *Inorg. Biochem.* **2006**, *100*, 1487-1494.
49. Marzilli, L.G. *New J. Chem.* **1990**, *14*, 409.
50. Pyle, A.M.; Rehman, J.P.; Meshoyrer, R.; Kumar, C.V.; Turro, N.J; Barton, J.K. *J. Am. Chem. Soc.* **1989**, *111*, 3051.
51. Wolfe, A.; Shimer, G.H.; Meehan, T. *Biochemistry.* **1987**, *26*, 6392.
52. Fangman, W. L., *Nucleic Acids Res.* **1978**, *5*, 653.